Chiral spin currents and spectroscopically accessible single merons in quantum dots

Catherine J. Stevenson and Jordan Kyriakidis*

Department of Physics and Atmospheric Science, Dalhousie University, Halifax, Nova Scotia, Canada B3H 3J5

(Received 14 July 2011; published 1 August 2011)

We provide unambiguous theoretical evidence for the formation of correlation-induced isolated merons in rotationally symmetric quantum dots. Our calculations rely on neither the lowest-Landau-level approximation, nor on the maximum-density-droplet approximation, nor on the existence of a spin-polarized state. For experimentally accessible system parameters, unbound merons condense in the ground state at magnetic fields as low as $B^* = 0.2$ T and for as few as $N = 3$ confined fermions. The fourfold degenerate ground state at B^* corresponds to four orthogonal merons $|QC\rangle$ characterized by their topological chirality C and charge Q. This degeneracy is lifted by the Rashba and Dresselhaus spin-orbit interaction, which we include perturbatively, yielding spectroscopic accessibility to individual merons. We further derive a closed-form expression for the topological chirality in the form of a chiral spin current and use it to both characterize our states and predict the existence of other topological textures in other regions of phase space, for example, at $N = 5$. Finally, we compare the spin textures of our numerically exact meron states to ansatz wave functions of merons in quantum Hall droplets and find that the ansatz qualitatively describes the meron states.

DOI: 10.1103/PhysRevB.84.075303 PACS number(s): 73.21.La, 31.15.V−, 75.25.−j, 03.65.Vf

I. INTRODUCTION

Spin states of electrons confined in semiconductor quantum dots (QDs) are an appealing platform for quantum information science due to their long dephasing times and controllability.[1–4] States used for this implementation must be long lived relative to the time scales required to flip a qubit, and remain coherent despite system perturbations. Topological states are promising candidates in that they are expected to have long decoherence times due to their *global* correlations and be robust against local perturbations.[5]

Skyrmions and merons are examples of topological spin textures that are predicted to form in two-dimensional (2D) electron systems.[6,7] Skyrmion excitations in bulk 2D systems have been predicted in the $\nu = 1$ quantum Hall regime,[6–8] and can condense into the ground state away from $\nu = 1$.[9] Experimental evidence supports the existence of skyrmion spin textures in GaAs/AlGaAs quantum wells.[10–13]

A meron can be described as half a skyrmion; it contains a central spin oriented perpendicular to the 2D plane, which transitions smoothly into in-plane winding away from the central spin. Unbound merons are not low-energy states in bulk 2D systems due to the prohibitive exchange energy of the in-plane winding. In finite-sized systems, such as the QDs we are considering in the present work, the textures are stabilized, and as we show below, they can condense in the ground state. Recent literature predicts the formation of merons in confined systems such as QDs in large magnetic fields.[14–16]

In this work, we use configuration-interaction techniques to study a fully interacting QD system to provide conclusive evidence for the formation of merons in the ground state. We find that merons form in systems containing as few as three particles,[17] at magnetic fields as low as 0.2 T, and away from the maximum density droplet regime. These states are degenerate. However, we show how this degeneracy can be lifted, and provide a method for predicting when merons will form in QD systems.

II. CHIRALITY

The chirality $C_n(\mathcal{C})$ of a vector field $\boldsymbol{v}(s)$ over a closed curve $\mathcal{C}$ in the direction of the unit vector $\boldsymbol{n}$ can be defined as

$$C_n(\mathcal{C}) = \oint_{\mathcal{C}} ds\, \frac{\boldsymbol{n}\cdot[\boldsymbol{v}(s)\times\partial_s\boldsymbol{v}(s)]}{|\boldsymbol{v}_\perp(s)|^2}, \tag{1}$$

where $\boldsymbol{v}_\perp(s) \equiv \boldsymbol{n}\times\boldsymbol{v}(s)$ is perpendicular to $\boldsymbol{n}$ and serves as a normalization factor; it is the global chiral character of the vector field in which we are chiefly interested.

We confine ourselves to two-dimensional, rotationally symmetric QDs centered at the origin, and we take the curve $\mathcal{C}$ to be a circle about the origin with radius r. Furthermore, we take our direction $\boldsymbol{n}$ to be perpendicular to the plane of the QD. Our vector field is the spin density $\boldsymbol{S}(\boldsymbol{r}) \equiv \langle\hat{\boldsymbol{S}}(r,\theta)\rangle$. Taking the QD to lie in the x-y plane, Eq. (1) takes the form

$$C_z(r) = \frac{1}{2\pi}\int_0^{2\pi} d\theta\, \frac{\boldsymbol{z}\cdot[\boldsymbol{S}(r,\theta)\times\partial_\theta\boldsymbol{S}(r,\theta)]}{|\boldsymbol{S}_\perp(r,\theta)|^2}, \tag{2}$$

where $\boldsymbol{S}_\perp(r,\theta) = \boldsymbol{z}\times\boldsymbol{S}(r,\theta)$.

We express our spin-density operator as

$$\hat{\boldsymbol{S}}(\boldsymbol{r}) = \sum_{\sigma,\sigma'}\hat{\psi}^\dagger_\sigma(\boldsymbol{r})\hat{\boldsymbol{\sigma}}_{\sigma\sigma'}\hat{\psi}_{\sigma'}(\boldsymbol{r}), \tag{3}$$

where $\hat{\psi}^\dagger_\sigma(\boldsymbol{r})$ is the field operator creating a fermion with spin $\sigma/2$ ($\sigma = \pm 1$) at position $\boldsymbol{r}$ and $\hat{\boldsymbol{\sigma}}$ is the vector of Pauli matrices. The chirality then takes the form of a chiral spin current

$$C_z(r) = \frac{1}{2\pi}\int_0^{2\pi} d\theta\, j_{\rm spin}(r,\theta), \tag{4}$$

with the chiral spin current density given by

$$j_{\rm spin}(r,\theta) = \frac{i}{2|S_+|^2}(S_+\partial_\theta S_+^* - S_+^*\partial_\theta S_+), \tag{5}$$

where $S_+ = \langle\hat{\psi}^\dagger_\uparrow(\boldsymbol{r})\hat{\psi}_\downarrow(\boldsymbol{r})\rangle$. As an example, consider the state $|\psi\rangle = (|L_z\, S_z\rangle + \gamma|L'_z\, S'_z\rangle)/\sqrt{2}$, where $|L_z^{(\prime)}\, S_z^{(\prime)}\rangle$ is a

general, correlated N-particle state with orbital angular momentum (z component) $L_z^{(\prime)}$ and spin angular momentum (z component) $S_z^{(\prime)}$. For these particular states $|\psi\rangle$, Eq. (4) yields

$$C_z(r) = (L_z' - L_z)(S_z - S_z')\delta_{|S_z - S_z'|,\,1}. \tag{6}$$

Perhaps not surprisingly, states of different orbital and spin angular momentum must be combined to produce a global chirality. C_z is an integer winding number whose magnitude indicates the number of full 2π rotations along a closed curve $\mathcal{C}$ about the QD origin, and whose sign indicates the sense of rotation. In the interacting system, such windings can spontaneously occur at points of degeneracy in the spectrum. (Both spin and a component of orbital angular momentum are conserved in our system.) We show below that this can occur in parabolic QDs containing three strongly interacting fermions at a point of fourfold degeneracy. We further show that the spin-orbit interaction splits this degeneracy into four spectroscopically distinct merons $|QC\rangle$ with $Q,C = \pm 1$.

III. THEORY

Our system consists of N interacting fermions of charge e, bound to a 2D plane and laterally confined by a parabolic potential. The 2D Hamiltonian used to describe this "standard model" is

$$\hat{\mathcal{H}} = \sum_i^N \hat{h}_i + \frac{1}{2}\sum_{i\neq j}^N \frac{e^2}{\epsilon|\hat{\boldsymbol{r}}_i - \hat{\boldsymbol{r}}_j|} + \hat{H}_{SO}, \tag{7a}$$

where ϵ is the dielectric constant of the medium and $\hat{h}$ is the single-particle Hamiltonian describing harmonic confinement in a perpendicular magnetic field:

$$\hat{h} = \frac{1}{2m^*}\widehat{P}^2(\hat{\boldsymbol{r}}) + \frac{1}{2}m^*\omega_0^2\hat{r}^2 + g\mu_B\hat{S}_z B_z, \tag{7b}$$

where $\hat{\boldsymbol{r}} = (\hat{x},\hat{y})$ is the position operator, m^* is the effective mass, and ω_0 is the parabolic confinement frequency. We work in a finite magnetic field perpendicular to the plane of the QD, and so $\widehat{\boldsymbol{P}} = \hat{\boldsymbol{p}} + \frac{e}{c}\boldsymbol{A}(\hat{\boldsymbol{r}})$, with $\boldsymbol{A}(\hat{\boldsymbol{r}}) = \frac{B}{2}(-\hat{y},\hat{x},0)$ in the symmetric gauge. The final term in Eq. (7b) is the Zeeman energy and plays no significant role in what follows due to the relatively small magnitude of both the g factor ($g \approx -0.44$ in GaAs) and the magnetic field ($B < 1$ T). The final term in Eq. (7a) is the spin-orbit interaction, which we deal with perturbatively in a subsequent section. In what follows, we fix the material parameters in Eq. (7) to typical values for GaAs heterostructures: $m^* = 0.067m_e$, $\epsilon = 12.4$, and $\hbar\omega_0 = 1$ meV.[18–20] Finally, we take $\hbar/2 = 1$.

Neglecting for now the spin-orbit interaction, we obtain the correlated eigenstates and the energies of Eq. (7) by configuration-interaction methods. The single-particle system, Eq. (7b), can be solved exactly yielding the well-known Fock-Darwin spectrum[21] with states $|mns\rangle$ labeled by harmonic oscillator numbers $m,n = 0,1,2,\ldots$, and spin $s = \pm 1/2$. We use these states to build up a basis of antisymmetrized many-body states, and write the Hamiltonian as a block-diagonal matrix with blocks segregated by the conserved quantities of particle number N, total spin S, z component of spin S_z, and orbital angular momentum L_z.

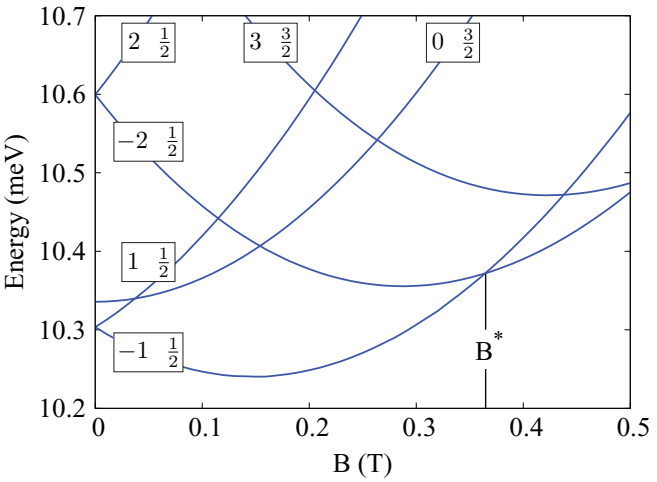

FIG. 1. (Color online) Low-lying spectra for $N = 3$ interacting particles with 2D harmonic confinement, Eq. 7. L_z and S quantum numbers are displayed for each state. The field B^* at which merons form in the ground state is marked.

The simplest system exhibiting meron textures occurs already for $N = 3$ confined particles. The low-lying spectrum is shown in Fig. 1. For the system parameters given above, a ground-state degeneracy exists at a field of $B^* = 0.365$ T. This degenerate manifold is spanned by the four spin-1/2 states $|L_z,S_z\rangle = |-1,\pm 1/2\rangle, |-2,\pm 1/2\rangle$. In the harmonic oscillator basis, these correlated states typically contain several thousand Hartree-Fock states in order to reach convergence in the energies to within 0.05%.

IV. MERON TEXTURES

The degenerate ground-state subspace at B^* described above contains merons. An explicit form that is important in what follows is

$$|QC\rangle = \frac{1-C}{2\sqrt{2}}\left(\left|-1,\frac{1}{2}\right\rangle - i\,Q\left|-2,-\frac{1}{2}\right\rangle\right) + \frac{1+C}{2\sqrt{2}}\left(\left|-1,-\frac{1}{2}\right\rangle + Q\left|-2,\frac{1}{2}\right\rangle\right). \tag{8}$$

These four states for $C = \pm 1$, $Q = \pm 1$ are orthogonal and yield the spin textures $\langle\hat{\boldsymbol{S}}(\boldsymbol{r})\rangle$ shown in Fig. 2. These spin textures are plotted using the real-space wave functions of the 2D harmonic trap.[22] Previous work[14–16] has focused on lowest-Landau-level physics or on semiclassical approximations. The present numerically exact results show that merons can exist far beyond the semiclassical regime; right down to the extreme quantum limit of very few confined particles where correlations are strongest. In particular, the three-particle ground states shown in Fig. 2 are *not* spin-polarized states, nor do they correspond to the $\nu = 1$ maximum density droplet. The states in Fig. 2 correspond to a filling factor of $2 > \nu > 1$. [The angular momentum of the N-particle maximum density droplet is $L_z = -N(N-1)/2$.]

A semiclassical (SC) ansatz for a single meron in a quantum Hall droplet is given in Ref. 16 in terms of spinors and Laughlin wave functions. Figure 3 shows a direct comparison between the spin textures $\langle\boldsymbol{S}(\boldsymbol{r})\rangle$ for the $|QC\rangle = |1\,1\rangle$ meron presented

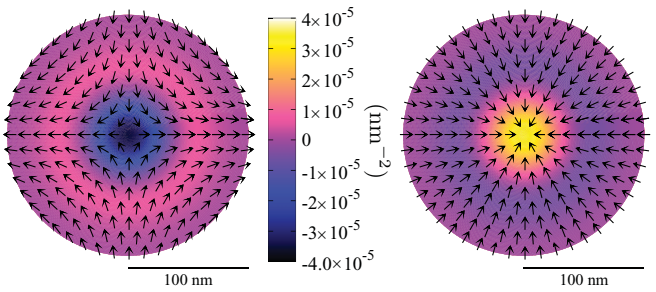

FIG. 2. (Color online) Two of the four meron textures for the three-particle states given in Eq. (8). The spin densities $\langle S_x(\boldsymbol{r})\rangle$ and $\langle S_y(\boldsymbol{r})\rangle$ are represented by the vector field, while $\langle S_z(\boldsymbol{r})\rangle$ is represented by the color bar. The remaining two configurations are obtained from these by a local in-plane spin rotation of π. The textures shown were obtained at the fourfold degeneracy point $B = B^*$ (see Fig. 1).

here and the SC ansatz for $N = 3$. Results are shown in units of $\ell_0 \equiv \sqrt{\hbar/2m^*\omega}$, where $\omega \equiv \sqrt{\omega_0^2+\omega_c^2/4}$, and ω_c is the cyclotron frequency. The two chief distinctions between the curves are the relative suppression of both charge (primarily at the origin) and spin polarization throughout the dot in the present work. Both effects can be attributed to the strong correlation effects captured in the present treatment. The suppression of charge at the origin is a result of the greater repulsion among the particles. The correlation-induced mixing among numerous Landau levels and angular-momentum and spin-resolved Slater determinants likewise has the effect of reducing the spin polarization throughout the dot. Indeed we find a conspicuous lack of full polarization throughout the dot.

V. SPIN-ORBIT COUPLING

To linear order, the spin-orbit interaction splits the degeneracy among the four merons states $|QC\rangle$. Remarkably, we find the Rashba term couples only to merons with positive chirality, whereas the Dresselhaus term couples only to those

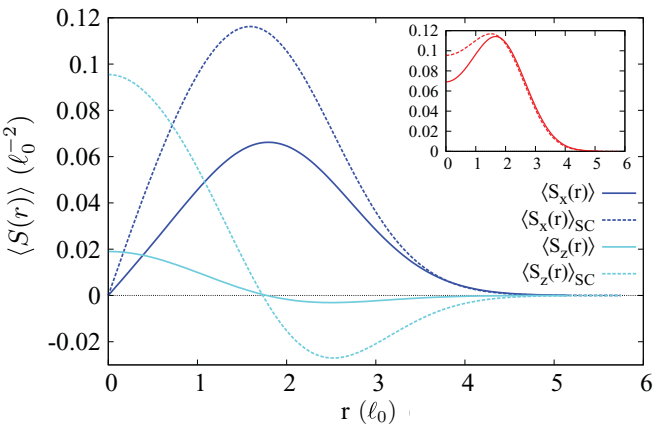

FIG. 3. (Color online) Comparison of spin density components for meron $|QC\rangle = |1\,1\rangle$ of Eq. (8) (solid lines) and the semiclassical result of Ref. 16 (dashed lines) for $\theta = 0$. The $S_x(r)$ curves vanish at the origin, and $S_y(r)$ is zero in both cases here. Inset: Particle density for the $|1\,1\rangle$ meron (solid) and semiclassical (dashed) result.

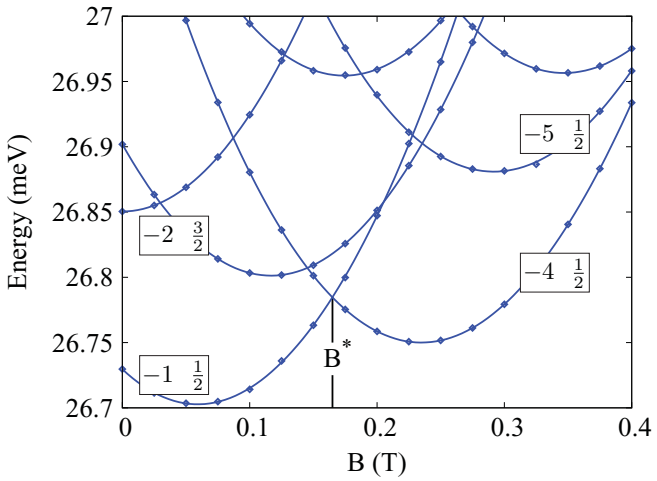

FIG. 4. (Color online) Low-lying spectra for $N = 5$ interacting particles with 2D harmonic confinement, Eq. 7. The quantum numbers L_z and S of selected levels are shown. B^* marks the field at which merons form in the ground state.

with negative chirality. Explicitly, the linearized spin-orbit interaction may be written as[23–29]

$$\hat{H}_{SO} = \beta(-\sigma_x P_x + \sigma_y P_y) + \alpha(\sigma_x P_y - \sigma_y P_x), \qquad (9)$$

where α and β are the Rashba and Dresselhaus spin-orbit coupling strengths, respectively. Within the lowest-energy degenerate subspace, the spin-orbit-induced energy splittings E_{QC} associated with each state $|QC\rangle$ are

$$E_{QC} = \frac{\mathcal{E}_C Q}{2}\left[(1+C)\alpha + (1-C)\beta\right], \qquad (10)$$

where

$$\mathcal{E}_C = \lambda\left\langle -2, \frac{C}{2}\left|\left[\left(1-\frac{1}{\nu}\right)\hat{S}_C\,\hat{b}^\dagger - \left(1+\frac{1}{\nu}\right)\hat{S}_C\,\hat{a}\right]\right| -1, -\frac{C}{2}\right\rangle, \qquad (11)$$

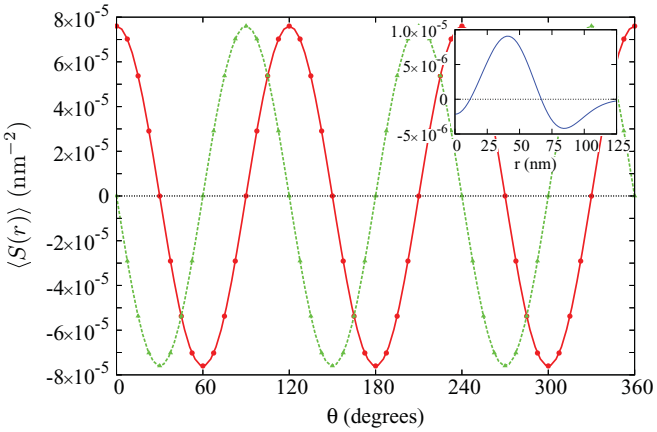

FIG. 5. (Color online) Meron spin texture $|QC\rangle = |1\ -3\rangle$ in the five-particle system at the degeneracy point B^* (Fig. 4). Plotted is $\langle S_x(r,\theta)\rangle$ (solid) and $\langle S_y(r,\theta)\rangle$ (dashed) around a closed curve at radius $r = 67$ nm. The winding number of 3 does not depend on r. Rather, the amplitudes decay with r due to the finite extent of the system. Inset: $\langle S_z(r)\rangle$ dependence on radius.

with $\lambda = 1/(\sqrt{2}\ell_0)$ and $Q,C = \pm$. Here, $\hat{a}$ and $\hat{b}^\dagger$ independently lower the orbital angular momentum of the $|L_z,S_z\rangle$ states, while $\hat{S}_\pm$ raises or lowers the spin. Also, $\nu = \sqrt{1+4\omega_0^2/\omega_c^2}$. Note if either α or β is zero, or if $\alpha = \beta$, a twofold degeneracy remains. Otherwise, the degeneracy is completely lifted. Since the Rashba term is to some extent tunable through externally applied gate voltages,[30–32] Eq. (10) demonstrates a measure of experimental control over the merons.

VI. PREDICTIONS

Equation (6) predicts that degenerate manifolds with states of different orbital and spin angular momentum contain quasitopological winding spin textures. Furthermore, the magnitude of the winding number associated with these states is equal to the difference between the orbital angular momentum of the degenerate states. In the case of a fourfold degeneracy, Eq. (8) generalizes to

$$|QC\rangle = \frac{1-c}{2\sqrt{2}}(|L_z,S_z\rangle - iq|L_z',S_z'\rangle) + \frac{1+c}{2\sqrt{2}}(|L_z,S_z'\rangle + q|L_z',S_z\rangle), \quad (12)$$

where $L_z \neq L_z'$, $|S_z - S_z'| = 1$, $c \equiv C/|C|$, and $q \equiv Q/|Q|$. The existence criteria for the quasitopological winding textures described by Eq. (12) is satisfied throughout the phase space of the QD. For example, Fig. 4 displays the lowest-lying spectrum for the five-particle system using the same experimental parameters listed above.

The fourfold degeneracy at $B^* = 0.16$ T occurs between the states $|L_z,S,S_z\rangle = |-1,1/2,\pm 1/2\rangle$ and $|-4,1/2,\pm 1/2\rangle$. According to Eq. (6), the quasitopological winding states that exist at this point have a winding of 3. Indeed this can be seen in Fig. 5, where the individual spin components for a meron state with QC quantum numbers $|QC\rangle = |1\ -3\rangle$ are plotted.

The large, off-center peak in the $\langle S_z(r)\rangle$ distribution is due to the increased Coulomb interaction strength relative to the three-particle system.

ACKNOWLEDGMENTS

This work was supported by the Natural Science and Engineering Research Council of Canada, by the Canadian Foundation for Innovation, and by the Lockheed Martin Corporation.

*jordan.kyriakidis@dal.ca; http://quantum.phys.dal.ca

[1] H. A. Engel, L. P. Kouwenhoven, D. Loss, and C. M. Marcus, Quant. Info. Proc. **3**, 115 (2004).
[2] J. M. Taylor, H. A. Engel, W. Dur, A. Yacoby, C. M. Marcus, P. Zoller, and M. D. Lukin, Nat. Phys. **1**, 177 (2005).
[3] S. Foletti, H. Bluhm, D. Mahalu, V. Umansky, and A. Yacoby, Nat. Phys. **5**, 903 (2009).
[4] E. A. Laird, J. M. Taylor, D. P. DiVincenzo, C. M. Marcus, M. P. Hanson, and A. C. Gossard, Phys. Rev. B **82**, 075403 (2010).
[5] S. Das Sarma, M. Freedman, and C. Nayak, Phys. Today **59**(7), 32 (2006).
[6] S. L. Sondhi, A. Karlhede, S. A. Kivelson, and E. H. Rezayi, Phys. Rev. B **47**, 16419 (1993).
[7] K. Moon, H. Mori, K. Yang, S. M. Girvin, A. H. MacDonald, L. Zheng, D. Yoshioka, and S. C. Zhang, Phys. Rev. B **51**, 5138 (1995).
[8] H. A. Fertig, L. Brey, R. Cote, A. H. MacDonald, A. Karlhede, and S. L. Sondhi, Phys. Rev. B **55**, 10671 (1997).
[9] L. Brey, H. A. Fertig, R. Côté, and A. H. MacDonald, Phys. Rev. Lett. **75**, 2562 (1995).
[10] S. E. Barrett, G. Dabbagh, L. N. Pfeiffer, K. W. West, and R. Tycko, Phys. Rev. Lett. **74**, 5112 (1995).
[11] E. H. Aifer, B. B. Goldberg, and D. A. Broido, Phys. Rev. Lett. **76**, 680 (1996).
[12] P. Khandelwal, A. E. Dementyev, N. N. Kuzma, S. E. Barrett, L. N. Pfeiffer, and K. W. West, Phys. Rev. Lett. **86**, 5353 (2001).
[13] G. Gervais, H. L. Stormer, D. C. Tsui, P. L. Kuhns, W. G. Moulton, A. P. Reyes, L. N. Pfeiffer, K. W. Baldwin, and K. W. West, Phys. Rev. Lett. **94**, 196803 (2005).
[14] S.-R. Eric Yang, N. Y. Hwang, and S. Park, Phys. Rev. B **72**, 165337 (2005).
[15] A. Petkovic and M. V. Milovanovic, Phys. Rev. Lett. **98**, 066808 (2007).
[16] M. V. Milovanovic, E. Dobardzic, and Z. Radovic, Phys. Rev. B **80**, 125305 (2009).
[17] For finely tuned spin-orbit parameters, merons can form at the fourfold degenerate singlet-triplet point in the $N = 2$ system, however only two of the four states have windings.
[18] P. N. Hai, W. M. Chen, I. A. Buyanova, H. P. Xin, and C. W. Tu, Appl. Phys. Lett. **77**, 1843 (2000).
[19] L. P. Kouwenhoven, N. C. Vandervaart, A. T. Johnson, W. Kool, C. J. P. M. Harmans, J. G. Williamson, A. A. M. Staring, and C. T. Foxon, Z. Phys. B **85**, 367 (1991).
[20] S. Tarucha, D. G. Austing, T. Honda, R. J. van der Hage, and L. P. Kouwenhoven, Phys. Rev. Lett. **77**, 3613 (1996).
[21] L. Jacak, P. Hawrylak, and A. Wojs, *Quantum Dots* (Springer-Verlag, Berlin, 1998).
[22] C. J. Stevenson and J. Kyriakidis, Phys. Rev. B **83**, 115306 (2011).
[23] G. Dresselhaus, Phys. Rev. **100**, 580 (1955).
[24] Yu. A. Bychkov and É. I. Rashba, Pis'ma Zh. Eksp. Teor. Fiz. **39**, 66 (1984) [JETP Lett. **39**, 78 (1984)].
[25] M. I. D'yakonov and V. I. Perel', Fiz. Tverd. Tela **13**, 3581 (1971) [Sov. Phys. Solid State **13**, 3023 (1972)].
[26] E. A. de Andrada e Silva, G. C. La Rocca, and F. Bassani, Phys. Rev. B **50**, 8523 (1994).
[27] E. A. de Andrada e Silva, G. C. La Rocca, and F. Bassani, Phys. Rev. B **55**, 16293 (1997).
[28] R. de Sousa and S. Das Sarma, Phys. Rev. B **68**, 155330 (2003).
[29] M. Florescu and P. Hawrylak, Phys. Rev. B **73**, 045304 (2006).
[30] J. Nitta, T. Akazaki, H. Takayanagi, and T. Enoki, Phys. Rev. Lett. **78**, 1335 (1997).
[31] G. Engels, J. Lange, T. Schapers, and H. Luth, Phys. Rev. B **55**, R1958 (1997).
[32] M. Studer, G. Salis, K. Ensslin, D. C. Driscoll, and A. C. Gossard, Phys. Rev. Lett. **103**, 027201 (2009).